JACS
JOURNAL OF THE AMERICAN CHEMICAL SOCIETY

COMMUNICATION

pubs.acs.org/JACS

Photoswitchable Nanoprobes Offer Unlimited Brightness in Frequency-Domain Imaging

Alexander D.Q. Li,[†,*] Chuanlang Zhan,[‡] Dehong Hu,[§] Wei Wan,[†] and Jiannian Yao[‡]

[†]Department of Chemistry and Center for Materials Research, Washington State University, Pullman, Washington 99164, United States
[‡]Beijing National Laboratory for Molecular Science, Institute of Chemistry, Chinese Academy of Sciences, Beijing 100190, P. R. China
[§]Pacific Northwest National Laboratory, Richland, Washington 99352, United States

Supporting Information

ABSTRACT: A single probe has limited brightness in time-domain imaging and such limitation frequently renders individual molecules undetectable in the presence of interference or complex cellular structures. However, a single photoswitchable probe produces a signal, which can be separated from interference or noise using photoswitching-enabled Fourier transformation (PFT). As a result, the light-modulated probes can be made super bright in the frequency domain simply by acquiring more cycles in the time domain.

Fluorescence imaging and fluorescence detection have contributed significantly to our understanding about single-molecule behavior and enzymatic dynamics.[1,2] Of particular importance is the brightness of fluorescent probes. To address such demands, quantum dots (QDs) have been recently developed. QDs emit about ~10−20 times brighter than single-molecule emitters and have many other advantages including tunable emission spectra and resistance to photobleaching.[3,4] A 5-nm CdSe QD, however, has a molar mass of ~228 kD, a factor of ~1000 larger than any dye molecules. The brightness per unit mass, an intensive property, does not increase. Therefore, the challenge, regarding to how to make ultrabright fluorescent probes without increasing their molar mass, remains unsolved. Moreover, there is still no current strategy to make fluorescent probes much brighter than QDs. Herein, we demonstrate that although such daunting tasks cannot be realized in the time domain, they readily become reality in the frequency domain for photoswitchable probes.

Using photoswitching, we found that modulated probes could be made superbright in frequency domain even though their time-domain intensity was limited. When a modulated probe emits the same number of photon as a nonmodulated interfering fluorophore does, their time-domain intensity is identical. However, their frequency domain intensity will be drastically different. Therefore, undesired fluorescent interference or noise can be mostly removed from the signal even when the interfering compounds fluoresce in the same color as the probe or emits orders of magnitude stronger than the modulated signal. Our results reveal that frequency-domain detection can potentially revolutionize fluorescence imaging.

To illustrate that periodically oscillating signals are superior to many other types, Figure 1 reveals the behavior of various signals

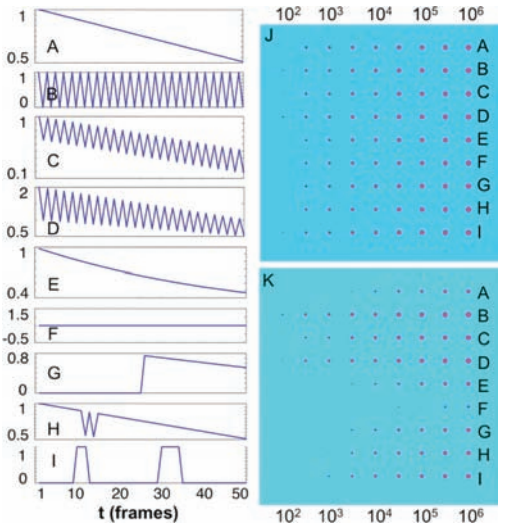

Figure 1. Periodically oscillating signals are superior to other forms. (A−I) Various behavior trajectories of fluorescent emitters are simulated, and their normalized intensities are plotted as a function of time. (J) Their nonzero (30th) frames with absolute intensities are displayed in the time domain. The spots in rows A−I represent one of the 50 frames defined in the A−I plots on the left, respectively. (K) Fourier transform (FT) of trajectories of different behavior reveals that only those periodic signals (B−D) are enhanced and amplified while all others (A and E−I) are significantly suppressed within limited periodic cycles.

(Figure 1A−I) in the time domain (Figure 1J) and frequency domain (Figure 1K). The fluorescent probes are simulated to decay linearly (Figure 1A), periodically (Figure 1B−D), or exponentially (Figure 1E). Time-domain signals may remain constant (Figure 1F), suddenly burst on (Figure 1G), serendipitously oscillate with the locked frequency ω_o (Figure 1H), or simply blink on and off during data acquisition. In the time domain, the 30th nonzero frame is displayed in Figure 1J with the maximum fluorescence intensity of all frames labeled on top of each column of spots. All fluorescent spots (rows A−I) appear in the image according to their intensity, no discrimination observed. However, photoswitching-enabled Fourier transform (PFT) converts time-domain images into frequency-domain images (Figure 1K), which selectively amplify the periodic signals yet suppress others.

Received: December 2, 2010
Published: May 03, 2011

dx.doi.org/10.1021/ja1108479 | J. Am. Chem. Soc. 2011, 133, 7628–7631

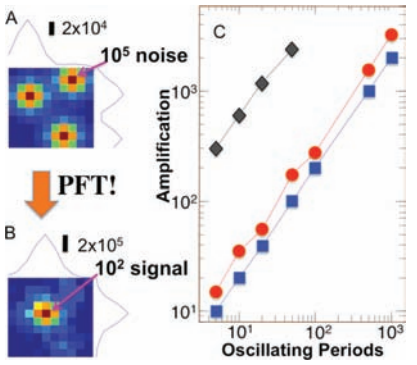

Figure 2. Signal amplification. (A) Interference (10^5 cps) completely floods the weak signal (10^2 cps) in time-domain imaging. (B) Frequency-domain imaging amplifies the central signal ≥4000 times (calculated on the basis of 1000/0.24 ≥ 4000), soaring above the interference. (C) Such amplification increases linearly with the oscillating cycles of the signals.

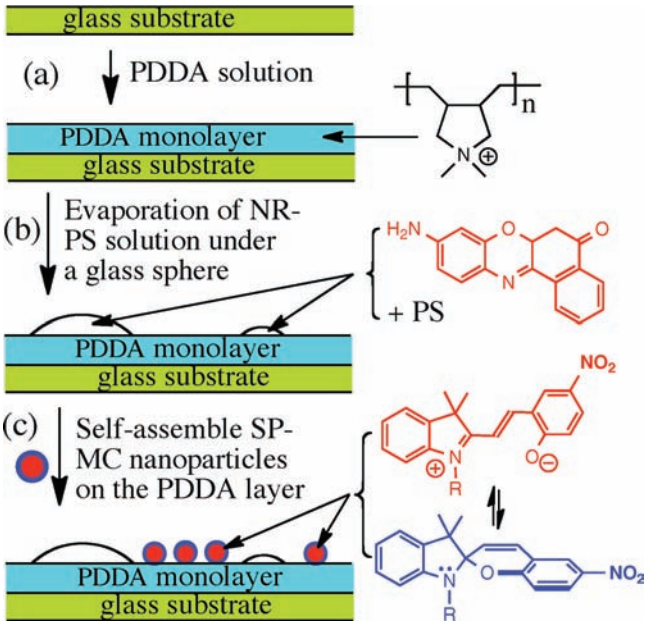

Figure 3. To compare the brightness side by side between modulated signals and non-modulated interfering fluorophores, we first assembled a monolayer of PDDA on a glass substrate (step a). PS patterns that contain interfering fluorophore Nile Red were deposited on top of this PDDA monolayer (step b). Where the PS polymer did not cover, SP−MC nanoparticles, which emit modulated signals, were self-organized because the negatively charged particles naturally were attracted to the positively charged PDDA layer (step c).

Most Fourier transform (FT) methods modulate the excitation light source to generate periodical signals in the same way as FTIR. For example, a silver nanodot when excited at 633 nm gives strong emission whose intensity can be modulated by adding a second 805-nm laser.[5] Later, this strategy of using a long-wavelength laser to modulate the emitting fluorophore intensity has been extended to FRET pairs.[6,7] Using FRET pairs to modulate the donor fluorescence has been reported previously.[8−10] However, PFT utilizes a constant excitation light source, yet relies on molecular structure changes in the sample to impart periodic signals. Thus, PFT is fundamentally different from conventional FT methods.

The image at the locked frequency (Figure 1K) differs radically from time-domain image (Figure 1J). Constant signals suffer the most loss (Figure 1F). The signals decaying linearly or exponentially disappear for maximum intensities of 10^2-10^3 cps and are considerably weakened for higher maximum intensities (Figure 1A and E). Sudden bursting-on or blinking on-and-off signals impart some noise carrying various frequency components, and therefore such patterned signals deteriorate moderately, although still near an order of magnitude (Figure 1G and I). Signals that serendipitously oscillate with the locked frequency for unknown reasons also experience great attenuation, demonstrating that the number of periodically modulated cycles is critically important. More importantly, all signals (Figure 1B−D) carrying the locked frequency thrive in the frequency-domain image (Figure 1K).

A signal with 10^2 cps residing next to three interfering fluorophores emitting 10^5 cps is completely inundated by the interference in time-domain imaging (Figure 2A). However, this weak signal is modulated with the locked frequency ω_o for 2500 periods, whereas the strong interference simply decays exponentially as for most fluorophores. When the data are transformed into frequency domain and displayed at the modulation frequency, the strong interference is powerfully suppressed into the noise, and the weak signal is significantly amplified (Figure 2B). The PFT imaging dramatically improves the interference-to-signal (I/S) ratio from undetectable levels I/S = 1000 to favorable I/S ratios of 0.15−0.24. Although signal modulation does not change the time-domain intensity, it dramatically boosts the frequency-domain intensity while suppressing all wrong-frequency components ($\omega \neq \omega_o$) including static zero-frequency (DC) contributions. In fact, measuring only five oscillations amplifies the periodic signal 10 times over linearly decaying interfering fluorophores, 15 times over exponentially decaying interfering fluorophores, and 300 times over constant interference (Figure 2C). The amplification is based on the oscillation amplitude, thus, no modulation, no enhancement. Therefore, the other key parameter that makes the periodic signals superior is the oscillation amplitude. Of particular importance is that the amplification scales linearly with the number of the modulated periods measured. As a result, a photoswitchable probe can be made super bright when unlimited periods are measured.

The unlimited frequency-domain brightness is originated from unlimited cycles at fixed time-domain brightness. To validate the super-brightness claims, we modulated photoswitchable spiropyran−merocyanine dyes to prove the principle. The photoswitchable spiropyran−merocyanine dyes were polymerized into polymeric nanoparticles using styrene, divinyl bezene, and butyl acrylate monomers. Because merocyanine (MC) emits red fluorescence and spiropyran (SP) has no emission in the red,[10,11] photoswitching of such dyes imparts on-and-off red-fluorescence ($\lambda_{max} \approx 665$ nm, Figure 3), a periodically oscillating signal mimicking the waveform in Figure 1B−D.[9,12] The merocyanine incorporated into the hydrophobic cores of the nanoparticles has improved quantum yield of $\Phi = 0.24$.[12] The chosen interfering fluorophore, Nile Red, emits at 636 nm with a quantum yield of $\Phi = 0.7$ (Figure 2A).[13] Both the interference and the signal fluoresce in the red, making it difficult to distinguish them on the basis of color only.

To localize the photoswitching signal from the interference, molecular self-assembly strategy and polymer patterns were used. First, a monolayer of PDDA (poly(dimethyldiallylammonium chloride) was self-assembled onto the glass coverslip from a 10 mM PDDA solution (step a in Figure 3) because positively

dx.doi.org/10.1021/ja1108479 |J. Am. Chem. Soc. 2011, 133, 7628–7631

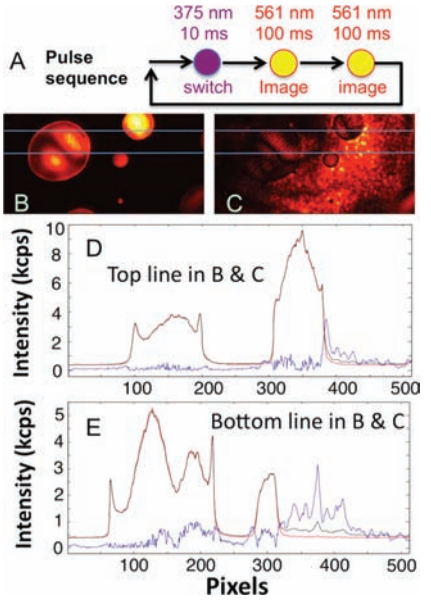

Figure 4. Frequency-domain imaging eliminates all interference. (A) A laser-switching-and-excitation cycle consists of one 375-nm photoswitching pulse, followed by two 561-nm imaging pulses. The switching laser converts spiropyran (SP) to merocyanine (MC), thus modulating fluorescence periods of bright and dark, but has no effect on nonswitching Nile Red (NR). (B) Time-domain imaging shows only the interfering NR in polymer circular patterns, and signals from MC outside of the polymer circular patterns are completely flooded and obscured. (C) Frequency-domain imaging reveals the modulated SP−MC in nanoparticles because modulated signals are amplified, but nonmodulated interference from NR is suppressed. (D and E) Line profiles in (B) and (C) confirm the amplified periodic signals (blue) and removal of the interference (red) devoid of modulation frequency (black and red).

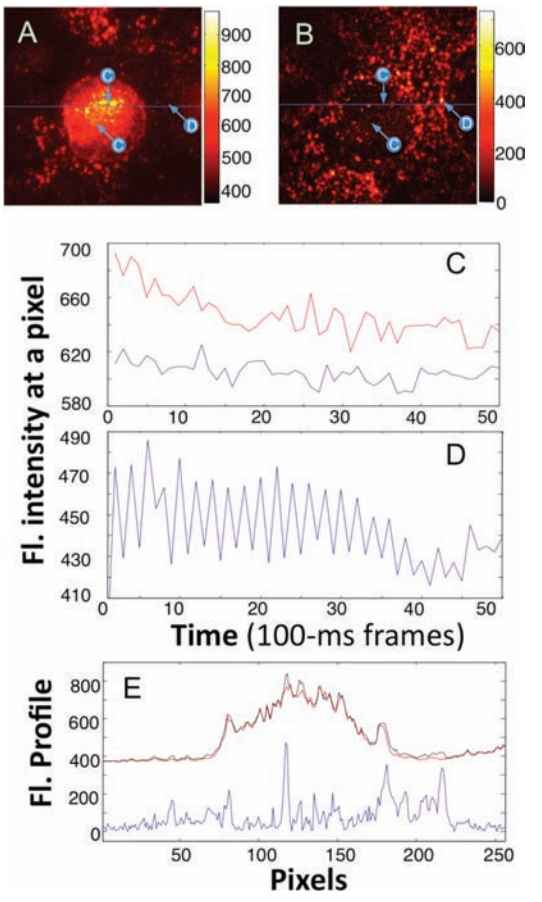

Figure 5. Weak signals emerge from overwhelming interference. The circular polymer pattern containing Nile Red in (A) is the brightest feature that obscures nanoparticles on or near it. However, PFT filters off linearly or exponentially decaying interference labeled with C in (A and B), whose profiles are displayed in (C), and reveals single-particle sensitivity in (B) because spiropyran−merocyanine nanoparticle signals are modulated with a unique locked frequency as labeled with D in (A and B) and plotted in (D). (E) Comparing time-domain with frequency-domain fluorescence intensity traces along the lines in (A) and (B) reveals that although interference dominates the time-domain data (red and black traces), single-molecule emitters can be detected in the presence of overwhelming interference (blue) in frequency domain.

charged polymers were attracted to the negatively charged silica surface.[14] Second, a toluene solution containing 0.5 μM Nile Red and 0.25 mg/mL PS (polystyrene) was evaporated on the coverslip under the curvature of a 60-mm-diameter glass sphere.[15] Under such conditions, the evaporation deposited micrometer-size PS circular patterns containing Nile Red at a concentration of 2 nmol/mg (step b in Figure 3). At this stage, the substrate was partially covered with hydrophobic PS patterns and the hydrophilic PDDA layer. Nanoparticles containing spiropyran−merocyanine dyes (SP−MC nanoparticles) self-organized in the regions where the PDDA layer was exposed, because such particles have negatively charged carboxyl groups and are naturally attracted to the positively charged PDDA monolayer (step c in Figure 3). Varying the particle concentration in solution controlled the coverage of the SP−MC nanoparticles.

The fluorescence intensity modulation under a single laser was enabled using one switching pulse followed by two probe pulses (Figure 4A). The photoswitching laser, which imparts photochemical conversion from spiropyran to merocyanine, was turned off during imaging. Therefore, all imaging series were acquired using a single 561-nm laser, which induced back-switching from the bright merocyanine to the dark spiropyran, thus causing intensity oscillation from frame to frame. The next results were that the signals from the probes in the time-domain images underwent alternating bright and dark cycles, whereas the interfering fluorophores experienced normal decays such as linear or exponential attenuation of fluorescence intensity.

Nile Red overloading made the PS patterns super bright, registering as high as 10,000 cps (Figure 4B) at 0.1 s bin. The SP−MC nanoparticles, however, emitted merely ~95 cps (0.1 s bin) at a locked frequency of ω_o = 2.32 Hz and were totally inundated by Nile Red. Therefore, one simply could not observe the nanoparticle signals in Figure 4B; all features originated from Nile Red dyes. Upon PFT, the ultrabright interference disappeared into the baseline, whereas the SP−MC-nanoparticle signals emerged as high as 3000 photon counts in the frequency-domain image (Figure 4C). The red and black curves in Figure 4D and E correspond to fluorescence intensity profiles before and after photoswitching, along the blue lines drawn in Figure 4 B and C. Obviously, the red and black curves trace each other over the ultrabright PS spots, confirming no modulation of the Nile Red intensity. Where the SP−MC nanopaticles are, fluorescence intensity modulation is barely visible (between 380 and 500 pixels in Figure 4D and 325−500 pixels in Figure 4E). Despite the weakly oscillating signals in time-domain imaging,

dx.doi.org/10.1021/ja1108479 |J. Am. Chem. Soc. 2011, 133, 7628–7631

the frequency-domain image reveals that the oscillating SP−MC signals are amplified many times over the Nile Red interference. Specifically, time-domain signals of 95 cps from merocyanine were augmented up to 3000 photon counts in the frequency domain because of integration over time, whereas the time-domain interference of 10,000 cps from Nile Red was reduced to ≤150 photon counts in the frequency domain. For strong signals, the I/S ratio of 13 was observed. For most signals, the I/S ratio improved dramatically from 75−150 in the time domain to ∼0.085 in the frequency domain, a factor of 880−1800 amplification. Such gain in signal and loss in noise between time and frequency domains make it possible to detect single-particle emitters against overwhelming fluorescence interference.

In time-domain imaging (Figure 5A), the circular PS areas such as the spots labeled as C are the brightest features in the image, rendering individual nanoparticles not observable (Figure 5A; labeled D). Frequency-domain imaging (Figure 5B), however, reveals vividly clear single-particle emitters (Figure 5B; labeled D). Specifically, pixels with intensity oscillating at the modulated frequency appear bright in frequency-domain imaging. Conversely, other pixels are dark in frequency-domain imaging (Figure 5B; spots labeled C). In Figure 5C, two interfering fluorophore trajectories are plotted. One interfering fluorophore (the red curve) follows exponential decay, while the other (the blue curve) decays linearly. Both oscillate randomly and contribute very little to the PFT intensity at $\omega_o = 2.32$ Hz. As a result, the corresponding interfering spots labeled C, though bright in the time domain (Figure 5A), are dark in the frequency domain (Figure 5B). In Figure 5D, a signal oscillating at 2.32 Hz is plotted. This signal labeled D in Figure 5A is much weaker than the Nile Red interference, but it becomes very bright in frequency-domain imaging (labeled D in Figure 5B). Fluorescence intensity profiles along the thin blue line in both Figure 5A and Figure 5B are plotted in Figure 5E. The red and black curves are fluorescence intensity before and after photoswitching. At this lower interfering scale, intensity modulation from the probes becomes more obvious and even nanoparticles on top of the PS circular pattern become visible. Still resolving single-particle emitters is difficult using time-domain data. In the frequency domain, however, resolution at individual particles is achieved after signal amplification and interference suppression.

The polymer-pattern experiments have validated the model simulation that photoswitching imparted modulation suppresses undesired noise and eliminates interference but amplifies periodic signals. Acquiring and accumulating data for long periods in the time domain cannot solve interference problems because intensity of interference does not fluctuate randomly and cancel itself. For example, summing over all 50 frames such as the one displayed in Figure 4B produced an image slightly worse than the single best frame in the 50-frame series because interference averaging outperformed signal averaging. However, the PFT method brings out the superiority of the probes that were modulated.

In this report, we demonstrate that periodically oscillating signals can be made super bright in frequency-domain imaging, even though the time-domain intensity has limited amplitude. Simulation and experimental data confirm that the PFT brightness scales with both the oscillation amplitude and the number of modulated periods. Thus, a new microscopy—photoswitching-enabled Fourier transform (PFT) fluorescence microscopy— is developed. PFT fluorescence microscopy has several advantages, including continuously amplifying the brightness of the modulated probes simply by measuring more oscillating cycles. Because of these advantages, such PFT microscopy is anticipated to have significant impacts in fluorescence imaging.

■ ASSOCIATED CONTENT

Supporting Information. Materials including nanoparticle synthesis and characterization and methods such as PFT data processing.This material is available free of charge via the Internet at http://pubs.acs.org.

■ AUTHOR INFORMATION

Corresponding Author
dequan@wsu.edu

■ ACKNOWLEDGMENT

We acknowledge the support of National Science Foundation (CHE-0805547). A portion of the research was performed using EMSL, a national scientific user facility sponsored by the Department of Energy's Office of Biological and Environmental Research and located at Pacific Northwest National Laboratory.

■ REFERENCES

(1) Lu, H. P.; Xie, X. S. *Nature* **1997**, *385*, 143.
(2) Lu, H. P.; Xun, L. Y.; Xie, X. S. *Science* **1998**, *282*, 1877.
(3) Chan, W. C. W.; Nie, S. M. *Science* **1998**, *281*, 2016.
(4) Bruchez, M.; Moronne, M.; Gin, P.; Weiss, S.; Alivisatos, A. P. *Science* **1998**, *281*, 2013.
(5) Richards, C. I.; Hsiang, J. C.; Senapati, D.; Patel, S.; Yu, J. H.; Vosch, T.; Dickson, R. M. *J. Am. Chem. Soc.* **2009**, *131*, 4619.
(6) Richards, C. I.; Hsiang, J. C.; Khalil, A. M.; Hull, N. P.; Dickson, R. M. *J. Am. Chem. Soc.* **2010**, *132*, 6318.
(7) Richards, C. I.; Hsiang, J. C.; Dickson, R. M. *J. Phys. Chem. B* **2010**, *114*, 660.
(8) Zhu, L. Y.; Zhu, M. Q.; Hurst, J. K.; Li, A. D. Q. *J. Am. Chem. Soc.* **2005**, *127*, 8968.
(9) Zhu, L. Y.; Wu, W. W.; Zhu, M. Q.; Han, J. J.; Hurst, J. K.; Li, A. D. Q. *J. Am. Chem. Soc.* **2007**, *129*, 3524.
(10) Tian, Z. Y.; Wu, W. W.; Wan, W.; Li, A. D. Q. *J. Am. Chem. Soc.* **2009**, *131*, 4245.
(11) Hu, D. H.; Tian, Z. Y.; Wu, W. W.; Wan, W.; Li, A. D. Q. *J. Am. Chem. Soc.* **2008**, *130*, 15279.
(12) Zhu, M. Q.; Zhu, L. Y.; Han, J. J.; Wu, W. W.; Hurst, J. K.; Li, A. D. Q. *J. Am. Chem. Soc.* **2006**, *128*, 4303.
(13) Nagy, K.; Gokturk, S.; Biczok, L. *J. Phys. Chem. A* **2003**, *107*, 8784.
(14) Lutt, M.; Fitzsimmons, M. R.; Li, D. Q. *J. Phys. Chem. B* **1998**, *102*, 400.
(15) Hong, S. W.; Xia, J. F.; Lin, Z. Q. *Adv. Mater.* **2007**, *19*, 1413.